Alexandria Engineering Journal (2015) 54, 415–422

HOSTED BY

Alexandria University

Alexandria Engineering Journal

www.elsevier.com/locate/aej
www.sciencedirect.com

ORIGINAL ARTICLE

Heat transfer enhancement in two-start spirally corrugated tube

Zaid S. Kareem [a], M.N. Mohd Jaafar [a], Tholudin M. Lazim [a,*], Shahrir Abdullah [b], Ammar F. AbdulWahid [a]

[a] Faculty of Mechanical Engineering, University Technology Malaysia, 81310 Skudai, Johor, Malaysia
[b] Department of Mechanical and Materials Engineering, Faculty of Engineering and Built Environment, University Kebangsaan Malaysia, 43600 Bangi, Selangor, Malaysia

Received 26 February 2015; revised 1 April 2015; accepted 5 April 2015
Available online 23 April 2015

KEYWORDS

Heat transfer enhancement;
Spiral corrugation;
Two-start;
Pressure drop;
Friction factor;
Laminar flow

Abstract Various techniques have been tested on heat transfer enhancement to upgrade the involving equipment, mainly in thermal transport devices. These techniques unveiled significant effects when utilized in heat exchangers. One of the most essential techniques used is the passive heat transfer technique. Corrugations represent a passive technique. In addition, it provides effective heat transfer enhancement because it combined the features of extended surfaces, turbulators and artificial roughness. Therefore, A Computational Fluid Dynamics was employed for water flowing at low Reynolds number in spiral corrugated tubes. This article aimed for the determination of the thermal performance of unique smooth corrugation profile. The Performance Evaluation Criteria were calculated for corrugated tubes, and the simulation results of both Nusselt number and friction factor were compared with those of standard plain and corrugated tubes for validation purposes. Results showed the best thermal performance range of 1.8–2.3 for the tube which has the severity of 45.455×10^{-3} for Reynolds number range of 100–700. The heat transfer enhancement range was 21.684%–60.5402% with friction factor increase of 19.2–36.4%. This indicated that this creative corrugation can improve the heat transfer significantly with appreciably increasing friction factor.

1. Introduction

Basically, three approaches are available yet to enhance the rate of heat transfer, active method, passive method and the compound method [1]. A power source is essential for the active, certain surface modifications or extension, and inserts or fluid additives are used in the passive method, while the compound method is a combination of the above two methods such as surface modification with fluid vibration [2].

* Corresponding author.
E-mail addresses: zaidsattar@yahoo.co.uk (Z.S. Kareem), nazri@mail.fkm.utm.my (M.N. Mohd Jaafar), tholudinlazim@yahoo.com (T.M. Lazim), shahrir@ukm.edu.my (S. Abdullah), ammar_alshoki@yahoo.com (A.F. AbdulWahid).
Peer review under responsibility of Faculty of Engineering, Alexandria University.

http://dx.doi.org/10.1016/j.aej.2015.04.001
1110-0168

Nomenclature

C_p	heat capacity at constant pressure
d	tube inside diameter
E	error
e	corrugation height
f	friction factor
F_s	safety factor
GCI	grid independence index
Gz	Graetz number
h	heat transfer coefficient
k	thermal conductivity
L	tube length
m	slope
Nu	Nusselt number
N	refinement ratio
P	pressure
p	pitch of corrugation
Pr	Prandtl number
PEC	performance evaluation criteria
q''	heat flux per unit area
R	tube inner radius
r	radial direction
Re	Reynolds number
T	temperature
u	fluid velocity
x	axial direction

Greek symbols

φ	severity index
ρ	density of fluid
v	kinematic viscosity of the fluid
μ	dynamic viscosity
θ	angular direction

Subscripts

*	dimensionless
b	bore
B	bulk
c	corrugated
en	envelope
in	inlet
n	nominal
out	outlet
s	smooth
x	local

Superscript

o	order of convergence

The motivation behind this activity is the desire to obtain more effective heat exchangers and other industrial applications [3], with the major objectives being to provide energy, material, and economic savings for the users of heat transfer enhancement technology.

In heat exchangers, corrugation and other surface modifications are commonly used because they are very effective in the heat transfer enhancement, also it is appearing very interesting for practical applications because it is a technique that promotes secondary recirculation flow, by inducing non-axial velocity components [4]. Recently, a swirl or helical flow pattern produced by employing surface modifications or any other passive technique for heat transfer enhancement is very interesting [5]. Also, Spiral corrugation increases heat transfer enhancement due to secondary flow swirls and surface curvatures pass by fluid layers, which also causes pressure losses [6].

There are few studies concerned with spirally corrugated tube. Mimura and Isozaki [7] investigated the effect of corrugations, different corrugation height and depth on friction factor and heat transfer. Withers [8,9] employed the analogy of heat, and momentum to correlate heat transfer and pressure drop expression in tubes, and the enhancement range of 2.5–3 was reported. Ganeshan and Rao [10] studied a single and multiple corrugation start on friction factor and heat transfer characteristics. Rounded corners corrugated ducts studied by Asako and Nakamura [11] to determine the characteristics of pressure drop and heat transfer. Laminar, transitional and turbulent flow in a tube with spiral flute was studied by Garimella et al. [12]. Their outcomes indicated that the most efficient in promoting the secondary flow are the fluted inner tubes. Thermal characteristics of corrugated tubes for different pitch values were studied by Rainieri and Pagliarini [13] which were used to enhance the convective heat transfer. Isothermal friction factor and heat transfer spiral corrugation of two start tubes with two-step tapes were studied by Zimparov [14]. A higher heat transfer coefficient and a friction factor were observed compared to the smooth tubes.

Experimental study of the effects of pitch-to-diameter ratio and rib-height to diameter ratios of tubes with helical corrugations on the rate of heat transfer was achieved by Pethkool et al. [15]. Their outcomes indicated that the corrugated tube's thermal performance is higher than those of the smooth tube. Spirally corrugated tubes were tested by Li et al. [16] numerically for the heat transfer evaluation. The corrugation gives better enhancement, which was concluded from their results depending on corrugation parameters of e/d and p/d.

Both friction factor and Nusselt number were experimentally studied by Saha [17]. His study covered the laminar region by employing circular duct having with a helical screw-tape insert.

Many researchers have investigated corrugated tubes before, and this study has been characterized by many features, the variable thermophysical properties of water one of them, which is the actual case of exchangers and gives results very close to the reality. In addition, a unique smooth corrugation profile was employed, and this kind of corrugation has no matches in the literature and supposes to show good thermal performance with minimum pressure drop which is the ultimate aim of all exchanger designers. Hence, the major objective of the current study was to determine the heat transfer enhancement and pressure drop characteristics of two-start spirally corrugated tube numerically, and also determine the effect of corrugation parameters e/d_n and p/d_n on heat transfer enhancement and pressure drop. This corrugation profile was chosen because it has smooth profile and can be made up at local markets with cheap price.

2. Geometrical configurations

Corrugated tubes are an interesting technique for obtaining efficient heat exchangers to reduced costs [18]. Hence, a 1 mm thickness aluminum tube of two-start spiral corrugation been modeled with configurations based on SolidWorks software. The main corrugation parameters are the corrugation height e, corrugation pitch p tube which has a variable envelope diameter d_{en} according to corrugation height e, and bore diameter d_b of 18 mm, as shown in Fig. 1. Five tubes were tested, each has a characteristic parameter of spiral corrugation height to diameter e/d_n, spiral corrugation pitch to diameter p/d_n and severity index $\varphi = e^2/(pd_n)$ as shown in Table 1.

Table 1 Corrugated tubes characteristics (all dimensions in mm).

Tube No.	d_n	e	p	e/d_n	p/d_n	φ
1	19	1	25	0.052632	1.315789	2.105×10^{-3}
2	19.5	1.5	21	0.076923	1.076923	5.495×10^{-3}
3	21	2	17	0.095238	0.809524	11.204×10^{-3}
4	21.5	2.5	13	0.116279	0.604651	22.361×10^{-3}
5	22	3	9	0.136364	0.409091	45.455×10^{-3}

3. Governing equations

The governing equation of the flow problem in the Cartesian coordinates system is as follows:

Conservation of mass:

$$\frac{\partial u_r}{\partial r}+\frac{u_r}{r}+\frac{1}{r}\frac{\partial u_\theta}{\partial \theta}+\frac{\partial u_x}{\partial x}=0 \tag{1}$$

Momentum equation r component

$$\rho\left(u_r\frac{\partial u_r}{\partial r}+\frac{u_\theta}{r}\frac{\partial u_r}{\partial \theta}-\frac{u_\theta^2}{r}+u_x\frac{u_r}{x}\right) = -\frac{\partial P}{\partial r}+\mu\left(\frac{\partial^2 u_r}{\partial r^2}+\frac{1}{r}\frac{\partial u_r}{\partial r}-\frac{u_r}{r^2}+\frac{1}{r^2}\frac{\partial^2 u_r}{\partial \theta^2}-\frac{2}{r^2}\frac{\partial u_\theta}{\partial \theta}+\frac{\partial^2 u_r}{\partial x^2}\right) \tag{2a}$$

Momentum equation θ component

$$\rho\left(u_r\frac{\partial u_\theta}{\partial r}+\frac{u_\theta}{r}\frac{\partial u_\theta}{\partial \theta}+\frac{u_r u_\theta}{r}+u_x\frac{\partial u_\theta}{\partial x}\right) = -\frac{1}{r}\frac{\partial P}{\partial \theta}+\mu\left(\frac{\partial^2 u_\theta}{\partial r^2}+\frac{1}{r}\frac{\partial u_\theta}{\partial r}-\frac{u_\theta}{r^2}+\frac{1}{r^2}\frac{\partial^2 u_\theta}{\partial \theta^2}+\frac{2}{r^2}\frac{\partial u_r}{\partial \theta}+\frac{\partial^2 u_\theta}{\partial x^2}\right) \tag{2b}$$

Momentum equation x component

$$\rho\left(u_r\frac{\partial u_x}{\partial r}+\frac{u_\theta}{r}\frac{\partial u_x}{\partial \theta}+u_x\frac{\partial u_\theta}{\partial x}\right) = -\frac{\partial P}{\partial \theta}+\mu\left(\frac{\partial^2 u_x}{\partial r^2}+\frac{1}{r}\frac{\partial u_x}{\partial r}+\frac{1}{r^2}\frac{\partial^2 u_x}{\partial \theta^2}+\frac{\partial^2 u_x}{\partial x^2}\right) \tag{2c}$$

Energy equation:

$$\rho c_p\left(u_r\frac{\partial T}{\partial r}+\frac{u_\theta}{r}\frac{\partial T}{\partial \theta}+u_x\frac{\partial T}{\partial x}\right)=k\left[\frac{1}{r}\frac{\partial}{\partial r}\left(r\frac{\partial T}{\partial r}\right)+\frac{1}{r^2}\frac{\partial^2 T}{\partial \theta^2}+\frac{\partial^2 T}{\partial x^2}\right] \tag{3}$$

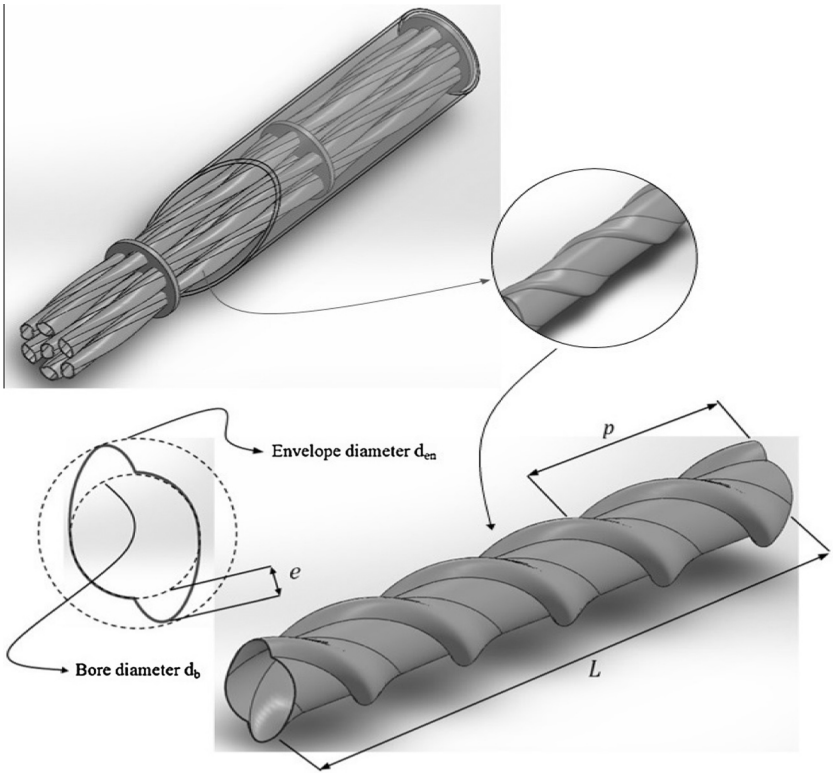

Figure 1 Two-start spirally corrugated tube configuration.

4. Numerical procedure

The commercial CFD code ANSYS FLUENT 14.0 was used to simulate the flow model of smooth and corrugated tubes with mesh generation performed by Gambit 2.4.6 mesh environment. The length of the tubes is 2 m, and the number of starts is two. Reynolds Number range is 100–1300, and the applied heat flux is 5000 (W m^{-2}), while the inlet temperature was set constant at 300 K. Water thermo-physical properties were set to be varied with temperature, i.e. μ, c_p, $\kappa = f(T)$. For determining the ordered discretization error in a *CFD*, Simulation's spatial convergence testing is a method of straightforward. The term of grid refinement study represents the same term of grid refinement study. As the grid is refined, i.e. cell of the grid becomes smaller in size, increase in number should asymptotically approach zero.

A uniform reporting of grid refinement research technique was obtained by Roache [19]. The measurement of the percentage resulted value is far from the value of the asymptotic numerical value that is called grid independence index, (*GCI)* which represents the criteria of solution changing with a further refinement of the grid, and the solution would be within the asymptotic range if indicated a small value.

To determine the optimum grids, four grids were examined at the same boundary conditions, coarse, medium, fine and finer. The grid independence index (*GCI)* for grids 1, 2, 3 and 4 was found to be 1.007, which is close to the range as shown in Fig. 2 and Table 2.

GCI is defined by

$$\left.\begin{aligned} GCI_{21} &= F_s \frac{E_{21}}{N_{21}^{o}-1} \\ GCI_{32} &= F_s \frac{E_{32}}{N_{32}^{o}-1} \\ GCI_{43} &= F_s \frac{E_{43}}{N_{43}^{o}-1} \end{aligned}\right\} \quad (4)$$

where E is the fractional error, F_s presents the safety factor, and N is refinement ratio, while o is the order of convergence. The numbers 1, 2, 3, 4... represent coarse, medium, fine, finer...etc., grids respectively. The value of 0.3 was recommended to the factor of safety F_s for the comparison between two grids, while for comparisons among two grids 1.25 was recommended.

Finite volume method is the tool which discretized the governing equations, then the implicit steady-state format was solved, and velocity and pressure fields were coupled by SIMPLE algorithm. Both first-order upwind and second-order upwind schemes were employed first, then after making sure that they give the same results (the deviation between them is 7.3×10^{-6}), first-order upwind scheme was chosen.

Table 2 Grid optimization.

Grid normalize	Grid spacing	Bulk temperature recovery (x = 1 m)
1	2	306.836
2	1	306.051
3	0.5	305.972
4	0.1	305.968

5. Results and discussion

5.1. Heat transfer results

The primary assessment criteria of laminar forced convective heat transfer performance were indicated by Nusselt number *Nu*. To validate the current simulation smooth tube data with previous studies, Churchil and Ozoe developed a closed form expression that covers both entrance and fully developed region [20] which is as follows:

$$Nu_x = \left[4.364\left(1+\left(\frac{Gz}{29.6}\right)^2\right)^{\frac{1}{8}}\right]\left[1+\left[\frac{Gz/19.04}{\left[1+(Pr/0.0207)^{2/3}\right]^{1/2}\left[1+(Gz/29.6)^2\right]^{1/3}}\right]^{3/2}\right]^{1/3} \quad (5)$$

where,

$$Gz = \frac{\pi}{4x_*} = [(\pi Re_{d_n} \cdot Pr)/4(x/d_n)] \quad (6)$$

Eq. (5) agrees within 5% with numerical data for $0.7 \leqslant Pr \leqslant 10$, and has the correct asymptotic behavior of large and small Gz and Pr. At a value of 1000 or less Gz represents the point of thermal fully developed. Another reliable correlation for laminar flow in smooth tube was proposed by Shah and London [21], which is empirical correlation and well known in the literature.

$$Nu = \begin{cases} 1.953(Re\ Pr\ D/L)^{1/3}; & (Re\ Pr\ d/L) \geqslant 33.3 \\ 4.364 + 0.0722 Re\ Pr \frac{D}{L}; & (Re\ Pr\ d/L) \leqslant 33.3 \end{cases} \quad (7)$$

The local heat transfer coefficient can be calculated as follows:

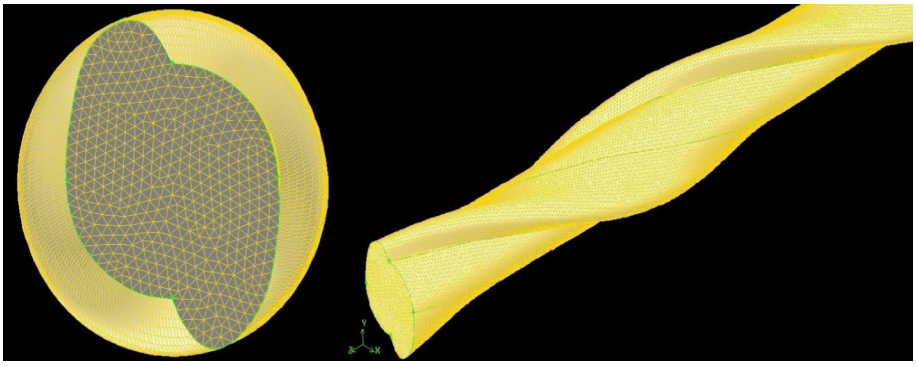

Figure 2 Computational mesh domain.

$$q''_s(x) = h(x)[T_W(x) - T_B(x)] \tag{8}$$

where q'' represents the heat flux, $T_w(x)$ and $T_B(x)$ are the local wall and bulk temperatures, respectively.

The local Nusselt number for the corrugated wall is defined as

$$Nu = hd_n/k \tag{9}$$

The Reynolds number is defined as

$$Re = \rho u d_n/\mu \tag{10}$$

where d_n is the nominal diameter, $d_n = (d_b + d_{en})/2$.

The results were compared with Eqs. (5) and (7) at Re of 100 for validation as shown in Fig. 3.

It was found that the deviation is less than ±3% and ±5% for Eqs. (5) and (7) respectively, which considered as acceptable, which indicates that the employed models, meshing, and numerical procedure for the simulation steps are also acceptable. The reasons of this deviation came from different sources, such as software residuals, mesh optimization and the error Margins of Eqs. (5) and (7).

Fig. 4 reveals the temperature and vorticity contours of the two-start corrugation tubes for different values of φ. The low wall temperature of the tube gives indication of the significant heat been transferred from the wall toward the fluid. The highest wall temperature was noted at $\varphi = 2.105 \times 10^{-3}$, while the lowest wall temperature observed at $\varphi = 45.455 \times 10^{-3}$ which gives a sign that the increase in severity leads to increase in the heat transfer due to swirls of fluid at the corrugation gap, and this swirls break the boundary layer, hence, reducing the resistance and prompting the thermal transportation.

As it was expected, the increase in the severity, causes increase in the swirls at secondary flow region, which is mixing fluid layers and increasing convective surface area as this figure showed, and the tube of high value of φ has a strong swirls, while the tube of the low value of φ has weak swirls and low thermal performance. Another merit for this kind of corrugation, is that the swirls do not disturb the core flow of the flow stream which is very important to decelerate the transition of the flow toward the turbulence region and reducing pressure drop.

Fig. 5 shows the comparison between local Nusselt number Nu_x and inversed Graetz number Gz^{-1} which is a function of (Pr, Re, and X/d_n) as it is mentioned in Eq. (5), where the Nu_x is in direct proportion with Gz^{-1}.

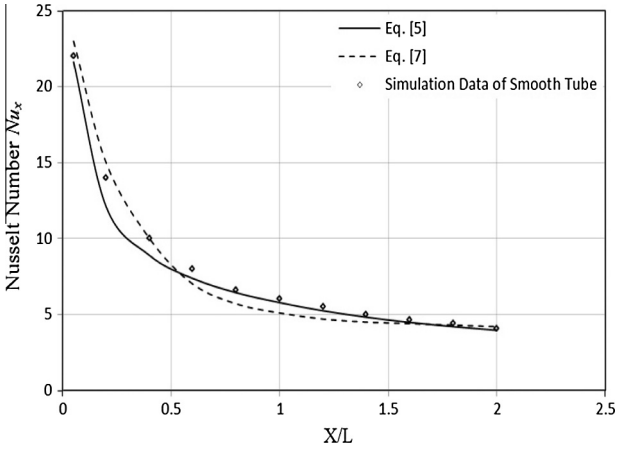

Figure 3 Nusselt number validation of current simulation data of the smooth tube with Eqs. (5) and (7).

This figure gives an evidence that Re has a dominant effect on Gz^{-1} among other parameters, and the enhancement of Nu_x is sufficient as Re increases from 100 to 1300. This figure shows two regions separated by line of slope $m = -0.833$, and the first region of low Re has accelerated increase in Nu_x values which ended at line of the following equation:

$$Nu_x = 21.833 - 0.833Gz^{-1} \tag{11}$$

The second region showed steady increase of Nu_x, which means the flow becomes uniform and stabilized, i.e., becomes fully developed flow after relatively long time and distance from the tube inlet because the effect of severity was not included in the figure but it has effect on the flow pattern; consequently, its effect reflected on Nu_x values. We have to mention that Fig. 5 indicates heat transfer enhancement in the range of 21.684%–60.5402% compared to smooth tube.

Fig. 6 shows average Nu against Re for different severity indexes φ. As mentioned before, severity combined the effects of all corrugation parameters in one expression except the parameter of the surface area parameter, which can be inferred from the enhanced Nu values.

This figure indicated that the Nu increases as φ increases especially at the region where $Re > 400$ because the severe roughness helps to disrupt the temperature field, the employed roughness represents a smooth repeated disturbance which acts as a swirls promoter for the fluid layers that are in contact with the tube wall, this leads to more heat transfer by mixing fluid layers with the main flow, and all of these reasons in addition to the extensive increase in the convective surface area reduce the retarding of the flow and increase heat transfer.

5.2. Pressure drop results

The drop in pressure was computed for the tube's entire length, and the laminar friction factor f of Darcy was given by the analytical as follows:

$$f = 64/Re \tag{12}$$

Recently, for the flow in corrugated tubes and tube, Barba [22] proposed a empirical correlation for laminar flow region of range $100 < Re < 800$, which is as follows:

$$f = 61.639Re^{-0.8602} \tag{13}$$

Fig. 7 shows the validation of friction factor f of the current simulation smooth tube data and a corrugated tube which subjected to the same loads and boundary conditions as it was employed in [22] with that of Eqs. (12) and (13) respectively, a good agreement was observed for the simulation data of smooth tube compared with Eq. (12), the deviation was ±2%, while, the deviation of simulation data of corrugated tube with Eq. (13) was ±5%, and the large deviation between the simulation data of corrugated tube with Eq. (13) came from many reasons: first, Eq. (13) correlated empirically for ethylene glycol fluid which has different thermophysical properties than water; second, Eq. (13) was derived for different p/d and e/d and also for different corrugation style and profile.

The friction factor f in comparison with Re presented in Fig. 8 for different values of severity φ. Obviously, when p/d_n decreases and e/d_n increases the friction factor will be

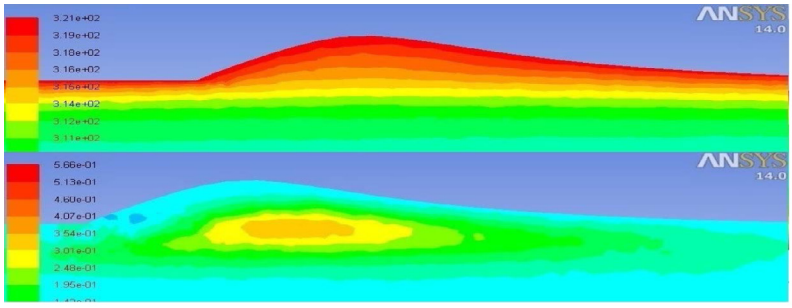

(a) Tube 1, $\varphi=45.455\times10^{-3}$

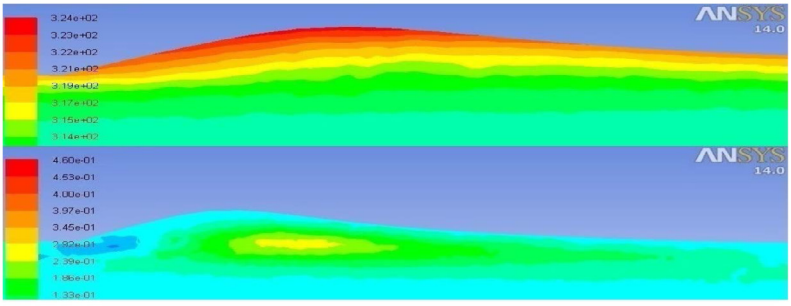

(b) Tube 2, $\varphi=22.361\times10^{-3}$

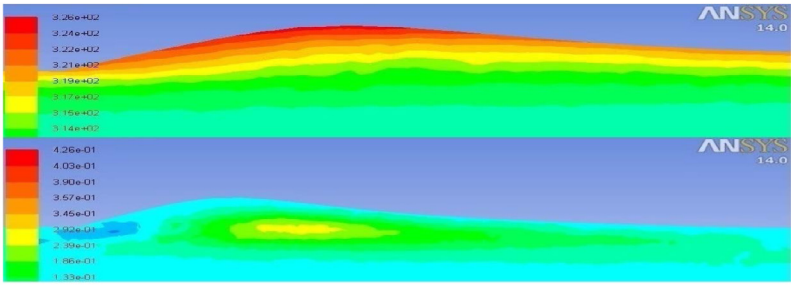

(c) Tube 3, $\varphi=11.204\times10^{-3}$

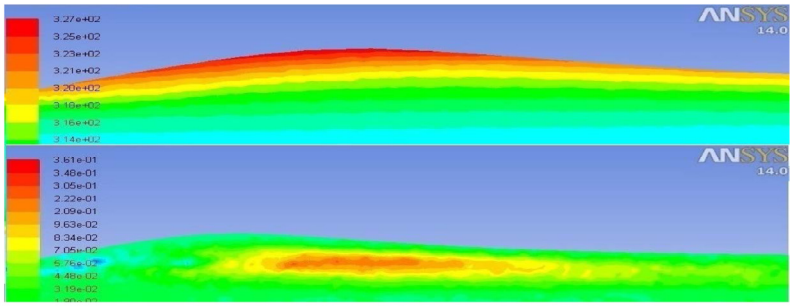

(d) Tube 4, $\varphi=5.495\times10^{-3}$

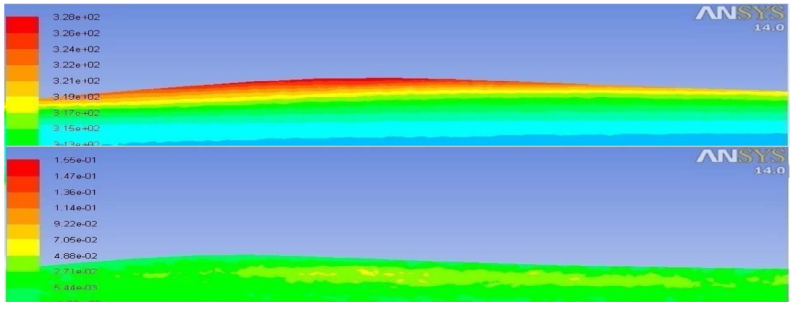

(e) Tube 5, $\varphi=2.105\times10^{-3}$

Figure 4 Temperature and vorticity contours for different values of severity.

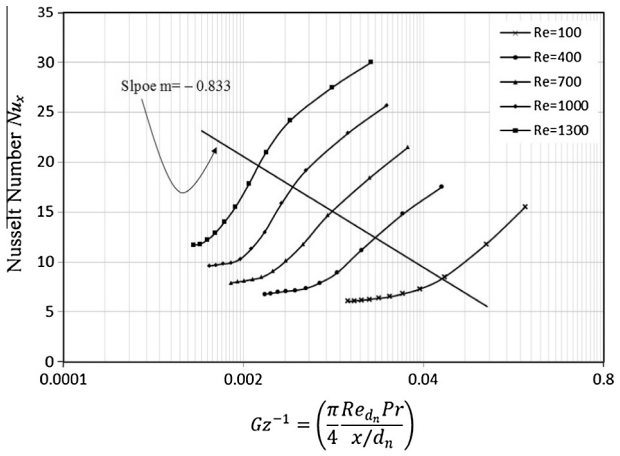

Figure 5 Nusselt number Nu_x against Graetz number Gz^{-1} for different Reynolds number.

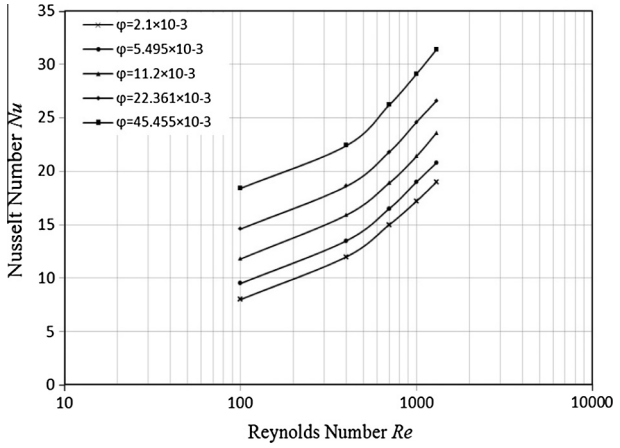

Figure 6 Average Nusselt number Nu against Reynolds number Re for different values of severity index φ.

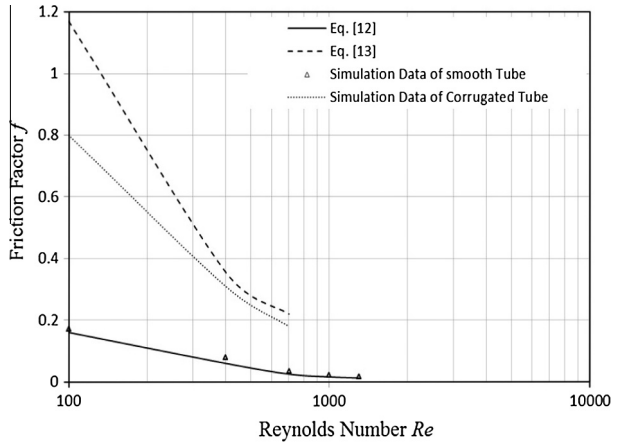

Figure 7 Friction factor f validation of the current simulation data with Eqs. (12) and (13).

increased at constant Re due to the increase in surface area representing by the corrugation surface area, i.e., as the volume that swept by working fluid increased the friction will increase. In addition, there will be more collisions between

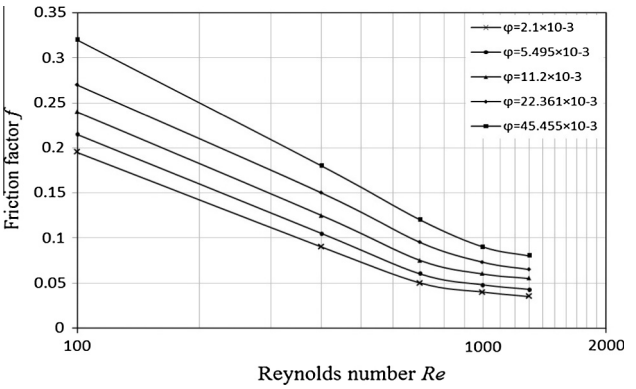

Figure 8 Friction factor f against the Reynolds number Re for different values of severity index φ.

fluid particles with the tube wall and also between fluid particles itself due to curvatures. This figure indicates reasonable values of f relative to other studies [18,23] because of the successive smooth curvy obstacles representing by corrugations which the current corrugations provided, and also, it offers harmony and orderly swirls at secondary flow region which helps to reduce pressure drop, hence, saving pumping power.

From the mentioned figure, as φ increases, the f increases because of deep corrugations which strengthens swirls. Another reasonable interpretation for the power dissipation is that perpendicular component of velocity vector (radial velocity component) to the main direction of flow causes significant retarding and its effect will increase as φ increases.

5.3. Criteria of performance

In order to assess the enhanced surfaces' effectiveness, the Economic criteria represent the major standard. In addition, Thermal and hydraulic standards have to be considered. Web [24] stated that to obtain perfect surface geometry for the flow in tube, the main influential variables the pressure drop, heat transfer rate and flow rate are used; furthermore, he reported a wide range of evaluation criteria based on convective area or other operational parameters.

The applicable criteria for most cases used by many researchers are the performance evaluation criteria (PEC); these criteria are defined as the heat transfer coefficient ratio of enhanced tube with a promoter to that of plain tube at constant pumping power [25].

$$i_E = (Nu_c/Nu_s)/(f_c/f_s)^{0.291} = f(Re_s) \tag{14}$$

Fig. 9 presents the performance evaluation criteria (PEC) against Re, and it shows the direct proportion of i_E with the increase in Re at φ of 2.105×10^{-3}, 5.495×10^{-3} and 11.204×10^{-3} for the Re range of < 700, then due to roughness effects of e/d_n and p/d_n that were included within φ the increase in friction factor becomes greater than the heat transfer obtained; hence, the friction effect will be dominating over the heat gain effect. From this figure, the best thermal performance 1.8–2.3 is for the tube which has φ of 45.455×10^{-3} for $100 < Re < 700$. This figure also shows an increase in f for the flow in a two-start spiral corrugated tubes for different φ values that were in the range of 19.2–36.4%.

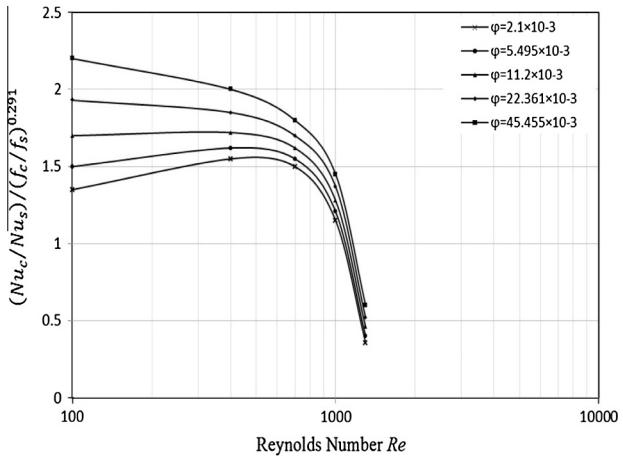

Figure 9 Performance evaluation criteria (*PEC*) against the Reynolds number *Re* for different values of severity index φ.

6. Conclusions

In this study, two-start spirally corrugated tubes were numerically studied to determine the effects of spiral corrugation characteristics e/d and p/d on overall thermal performance.

From the obtained results, it was found that this geometry with smooth spiral corrugations can improve the heat transfer significantly at low, medium Reynolds Number. While the region after *Re* of 700 has increase in friction factor much greater than the enhancement in heat transfer, it was concluded that the master key for getting better heat transfer with lowest pressure drop is the corrugation profile, and it has to be optimized to produce more heat transfer at lowest pumping power.

Results indicated that the severity index φ has a great effect on heat transfer enhancement and friction factor, and the heat gained accompanied with a pressure loss especially at high *Re*. Also it was concluded that this corrugation profile produced harmony and orderly swirls at secondary flow region which reduces the pressure drop sufficiently and saving pumping power. In addition, the tube of severity value of φ of 45.455×10^{-3} had the best thermal performance range of 1.8–2.3.

The heat transfer enhancement range is 21.684%–60.5402%, which means the tube geometry has a very good profile; hence, we can get a high value of heat transfer coefficient by using simple smart geometry, and the friction factor increase was found in the range of 19.2–36.4%, which is relatively acceptable compared to the gained heat transfer.

References

[1] S. Liu, M. Sakr, A comprehensive review on passive heat transfer enhancements in pipe exchangers, Renew. Sust. Energy Rev. 19 (2013) 64–81.
[2] V.P. Suhas, P.V. Babu, Heat transfer augmentation in a circular tube and square duct fitted with swirl flow generators: a review, Int. J. Chem. Eng. Appl. 2 (2011) 326–331.
[3] A.S. Dalkilic, S. Wongwises, Intensive literature review of condensation inside smooth and enhanced tubes, Int. J Heat Mass Transfer 52 (2009) 3409–3426.
[4] S. Rainieri, G. Pagliarini, Convective heat transfer to temperature dependent property fluids in the entry region of corrugated tubes, Int. J Heat Mass Transfer 45 (2002) 4525–4536.
[5] S. Rainieri, F. Bozzoli, L. Schiavi, G. Pagliarini, Numerical analysis of convective heat transfer enhancement in swirl tubes, Int. J. Numer. Meth. Heat Fluid Flow 21 (2011) 559–571.
[6] A.Z. Dellil, Numerical simulation of a spiral wall, Mechanika 20 (2014) 42–48.
[7] K. Mimura, A. Isozaki, Heat transfer and pressure drop of corrugated tubes, Desalination 22 (1977) 131–139.
[8] J.G. Withers, Tube-side heat transfer and pressure drop for tubes having helical internal ridging with turbulent/transitional flow of single-phase fluid. Part 1 single-helix ridging, Heat Transfer Eng. 2 (1980) 48–58.
[9] J.G. Withers, Tube-side heat transfer and pressure drop for tubes having helical internal ridging with turbulent/transitional flow of single-phase fluid. Part 1 single-helix ridging, Heat Transfer Eng. 2 (1980) 43–50.
[10] S. Ganeshan, M.R. Rao, Studies on thermohydraulics of single- and multi-start spirally corrugated tubes for water and time-independent power law fluids, Int. J. Heat Mass Transfer 25 (1982) 1013–1022.
[11] Y. Asako, H. Nakamura, Heat transfer and pressure drop characteristics in a corrugated duct with rounded corners, Int. J. Heat Mass Transfer 31 (1988) 1237–1245.
[12] S. Garimella, R.N. Christensen, Experimental investigation of fluid flow mechanisms in annuli with spirally fluted inner tube, ASHRAE Trans. 99 (1993) 1205–1216.
[13] S. Rainieri, G. Pagliarini, Convective heat transfer to orange juice in smooth and corrugated tubes, Int. J. Heat Technol. 15 (1997) 69–75.
[14] V. Zimparov, Enhancement of heat transfer by a combination of two-start spirally corrugated tubes with a twisted tape, Int. J. Heat Mass Transfer 44 (2001) 551–574.
[15] S. Pethkool, S. Eiamsa-Ard, S. Kwankaomeng, P. Promvonge, Turbulent heat transfer enhancement in a heat exchanger using helically corrugated tube, Int. Commun. Heat Mass. Transfer 38 (2011) 340–347.
[16] Y. Li, J. Wu, H. Wang, L. Kou, X. Tian, Fluid flow and heat transfer characteristics in helical tubes cooperating with spiral corrugation, Energy Procedia 17 (2012) 791–800.
[17] S.K. Saha, Thermohydraulics of laminar flow through a circular tube having integral helical corrugations and fitted with helical screw-tape insert, Chem. Eng. Commun. 200 (2013) 418–436.
[18] P.G. Vicente, A. Garcia, A. Viedma, Mixed convection heat transfer and isothermal pressure drop in corrugated tubes for laminar and transition flow, Int. Commun. Heat Mass. Transfer 31 (2004) 651–662.
[19] P.J. Roache, K.N. Ghia, F.M. White, Editorial policy statement on the control of numerical accuracy, J. Fluids Eng. 108 (1986) 2.
[20] A. Bejan, A.D. Kraus, Heat Transfer Handbook, John Wiley & Sons Inc., New Jersey, 2003.
[21] R.K. Shah, A.L. London, Laminar Flow Forced Convection in Ducts, first ed., Academic Press, Massachusetts, New York, 1978.
[22] A. Barba, S. Rainieri, M. Spiga, Heat transfer enhancement in corrugated tube, Int. Commun. Heat Mass. Transfer 29 (2002) 313–322.
[23] A. Garcia, J.P. Solano, P.G. Vicente, A. Viedma, The influence of artificial roughness shape on heat transfer enhancement: corrugated tubes, dimple tubes and wire coils, Appl. Therm. Eng. 35 (2012) 196–201.
[24] R.L. Web, Performance evaluation criteria for use of enhanced heat transfer surfaces in heat exchanger design, Int. J. Heat Mass Transfer 24 (1981) 715–726.
[25] H. Usui, Y. Sano, K. Iwashita, A. Isozaki, Enhancement of heat transfer by a combination of an internally grooved rough tube and a twisted tape, Int. Chem. Eng. 26 (1986) 97–104.